Mechanisms of serpentinization and some geochemical effects

Karthik Iyer

Dissertation for the degree of Doctor Scientiarum

Physics of Geological Processes

Faculty of Mathematics and Natural Sciences

University of Oslo

September 2007

Series of dissertations submitted to the
Faculty of Mathematics and Natural Sciences, University of Oslo.
No. 674

ISSN 1501-7710

Cover: Inger Sandved Anfinsen.
Printed in Norway: AiT e-dit AS, Oslo, 2007.

Produced in co-operation with Unipub AS.
The thesis is produced by Unipub AS merely in connection with the
thesis defence. Kindly direct all inquiries regarding the thesis to the copyright
holder or the unit which grants the doctorate.

Unipub AS is owned by
The University Foundation for Student Life (SiO)

Preface

The work presented in this thesis was carried out at Physics of Geological Processes (Department of Physics), University of Oslo from 2004 through 2007. The research was funded by a Centre of Excellence grant from the Norwegian Research Council to PGP.

I am indebted to my principal supervisor Professor Bjørn Jamtveit for the guidance and freedom that I had during my studies. I am equally grateful to my other supervisors, Professors Håkon Austrheim and Yuri Podladchikov, for the numerous scientific discussions and help I received throughout my time at PGP. My supervisors' constant encouragement and support helped make this Ph.D. possible.

I am also grateful for all the advice and knowledge imparted to me by Anders Malthe-Sørensson, Jens Feder, Joachim Mathiesen, Paul Meakin and Timm John whose contributions are presented in this thesis. I also thank Dani Schmid, Sergei Medvedev, Marcin Dabrowski and Anja Røyne for all of their 'unofficial' but invaluable help. All of the above mentioned people never once complained about the constant stream of questions I had for them and for that I am extremely thankful. I would also like to thank Muriel Erambert for all her assistance and insight during my long mineral analysis sessions at the EMP and our administrative secretary, Karin Brastad, who was always there to help sort out the little but important things.

My office- and flat-mates, in addition to everyone at PGP, provided me with an environment that was both, academically and socially, superb.

Lastly, I would like to thank my family and my other half, Yordanka, for all their love and support throughout my Ph.D., and more importantly, for believing in me.

Oslo, September 2007

Karthik Iyer

List of Scientific Manuscripts

I. Serpentinization of the oceanic lithosphere and some geochemical consequences: Insights from the Leka Ophiolite Complex, Norway. *Chemical Geology* (in review).

II. Reaction-assisted hierarchical fracturing during serpentinization. *Earth and Planetary Science Letters* (in review).

III. Joint spacing driven by differential volume expansion: The role of frictional sliding. *Manuscript*.

Contents

1 Introduction

Serpentinites occur in a variety of tectonic settings and are formed due to the hydration of mafic and ultramafic rocks. The process of serpentinization significantly alters the physical and chemical properties of the affected rock. One of the important effects of serpentinization is the change in density of the affected rocks. Complete serpentinization of a peridotite results in a water uptake of 13-15% by weight and a volume increase of around 40% (e.g. Schroeder et al., 2002; Shervais et al., 2005). These changes also influence the rheology of the rock and thus play an important role in the formation of detachment faults and strain localization along serpentinized fault planes (Escartín et al., 1997a, b). Serpentinization of ultramafic rocks reduces the seismic velocities and increases the magnetic susceptibility of peridotites which contributes to magnetic anomalies along the ocean floor. Serpentinization and deserpentinization processes in subduction zones affects the water budget of the subduction zone, intraplate fluid flow, mechanics of plate bending and the buoyancy of the subducting slab. In addition, serpentinization of peridotites may result in the metasomatism of the surrounding rocks (e.g. rodingitization), affects the global seawater-lithosphere chemical budgets and promotes the formation of mineral deposits on the ocean floor (e.g. Charlou et al., 2002; Tivey, 2007). Serpentinization occurring at hydrothermal systems results in the production of large amounts of CH_4 and H_2 in the vent fluids and can support a variety of life forms (e.g. Kelley et al., 2005).

Serpentinization is therefore an important metamorphic process which has far-reaching consequences on the petrophysical and geochemical properties of the oceanic lithosphere.

1.1 Serpentinites and serpentine minerals

Serpentinites are metamorphic rocks consisting primarily of serpentine minerals (lizardite, chrysotile and/or antigorite) with accessory phases like brucite, magnetite, and Mg and Ca-Al silicates (O'Hanley, 1996). Serpentinites are generally black or green in color while yellowish to reddish rocks contain significant amounts of clay minerals (Mével, 2003). Serpentine minerals are trioctahedral 1:1 layer silicates and consist of infinite sheets of 4-coordinated Si and 6-coordinated Mg (O'Hanley, 1996).

The general chemical formula for serpentine is $Mg_3Si_2O_5(OH)_4$. Si in the tetrahedral sheet may be substituted for Al and Fe^{3+} while Mg in the octahedral sheet may be substituted by Fe^{2+}, Fe^{3+}, Cr, Al, Ni and Mn (O'Hanley, 1996). The main serpentine minerals are distinguished by their crystal structure. Lizardite consists of planar layers (Fig. 1A) while chrysotile consists of scrolled layers which tend to form cylinders (Fig. 1B; O'Hanley, 1996; Mével, 2003). Antigorite possesses a modulated structure (Guggenheim and Eggleton, 1988) in which the 1:1 layer periodically reverses itself (Fig. 1C; O'Hanley, 1996). Lizardite is more susceptible to accept substitution than chrysotile and is more enriched in Al (Moody, 1976; O'Hanley, 1992; Mével, 2003). A lack of octahedral sites in antigorite results in a loss of Mg and $(OH)_4$ with respect to Si and is therefore more enriched in Si (Wicks and Whittaker, 1975; Uehara and Shirozu, 1985; Bailey, 1988). Phase calculations indicate that serpentine is stable below temperatures of 550°C and the stability is slightly enhanced at increasing pressures (O'Hanley, 1996).

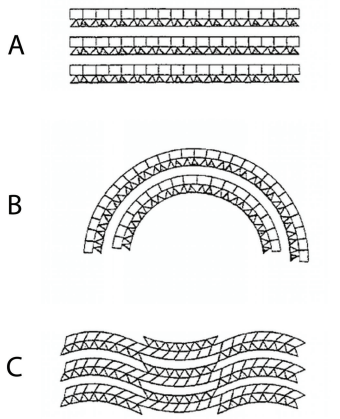

Figure 1. Sketch of crystallographic structures of serpentine minerals: A = lizardite, B = chrysotile; C = antigorite (From Mével, 2003).

1.2 Hydration reactions and serpentine formation in ultramafic rocks

Ultramafic rocks are composed predominantly of olivine, orthopyroxene and clinopyroxene. A number of reactions (R1-R7) can be used to describe the serpentinization of these minerals in the CaO-MgO-SiO_2-H_2O (CMSH) system. At water saturation, these reactions may take place over a wide-range of temperatures and are slightly dependent on pressures (Fig. 2). Fig. 3 shows the compositional space

(CaO-MgO-SiO_2) occupied by the reacting minerals (olivine, orthopyroxene and clinopyroxene) and their products (tremolite, talc, serpentine and brucite) during hydration reactions.

Amphiboles are less abundant in serpentinites with the most common variety being tremolite (Mével, 2003). The formation of tremolite in serpentinites is attributed to the breakdown of pyroxenes in the presence of water. The reaction of orthopyroxene and clinopyroxene with fluid results in the formation of amphibole at temperatures <800°C at 1kbar (R1).

$$2CaMgSi_2O_6 + 5MgSiO_3 + H_2O \rightarrow Ca_2Mg_5Si_8O_{22}(OH)_2 + Mg_2SiO_4 \quad (R1)$$

clinopyroxene + orthopyroxene + water = tremolite + olivine

Talc is commonly associated with the alteration of orthopyroxene (Mével, 2003). Orthopyroxene will completely react with excess fluids to form talc and olivine at temperatures of <650°C at 1kbar (R2) and has also been confirmed by experimental and theoretical observations (Pawley, 1998; Melekhova et al., 2006; Iyer et al., 2007a).

$$5MgSiO_3 + H_2O \rightarrow Mg_2SiO_4 + Mg_3Si_4O_{10}(OH)_2 \quad (R2)$$

orthopyroxene + water = olivine + talc

The talc formed in R2 reacts with olivine and fluid present in the rock to form antigorite (R3).

$$Mg_3Si_4O_{10}(OH)_2 + 6Mg_2SiO_4 + 9H_2O \rightarrow 5Mg_3Si_2O_5(OH)_4 \quad (R3)$$

talc + olivine + water = serpentine

Tremolite is stable at temperatures between 450°-825°C at $P_{total} = P(H_2O) = 5$ kbars whereas diopside is the stable calcium-bearing phase at higher and lower temperatures (Evans et al., 1976; Jenkins, 1983; Peacock, 1987). The tremolite produced by R1 is consumed at lower temperatures (<480°C) together with some olivine and water resulting in the formation of diopside and serpentine (R4).

$$Ca_2Mg_5Si_8O_{22}(OH)_2 + 6Mg_2SiO_4 + 9H_2O \rightarrow 2CaMgSi_2O_6 + 5Mg_3Si_2O_5(OH)_4 \quad (R4)$$

tremolite + olivine + water = diopside + serpentine

The direct hydration of olivine at low temperatures (<400°C at 1kbar) results in the formation of serpentine and brucite due to the excess Mg present in olivine compared to serpentine. Brucite is therefore found in serpentinized ultramafic rocks which contain significant amounts of olivine. Iron can substantially substitute magnesium in brucite resulting in ferroan brucite. Brucite occurs within the core of the mesh texture (see chapter 1.3) or within serpentine veins (Mével, 2003).

$$2Mg_2SiO_4 + 3H_2O \rightarrow Mg_3Si_2O_5(OH)_4 + Mg(OH)_2 \quad \text{(R5)}$$

olivine + water = serpentine + brucite

Magnetite is another accessory mineral commonly formed during the serpentinization of ultramafic minerals and is the product of the oxidation of the ferrous iron present in these minerals. The formation of magnetite is an important reaction as it may be associated with the generation of reduced volatile species such as H_2 and CH_4, and alteration of the magnetic properties of ultramafic rocks (see chapters 3.3 and 4).

At high pressures (>15 kbars), the sequence of reactions change and the hydration of olivine and orthopyroxene at such pressures would result in the direct formation of antigorite (R6 and R7; see O'Hanley, 1996; Pawley, 1998).

$$6MgSiO_3 + 3H_2O \rightarrow Mg_3Si_2O_5(OH)_4 + Mg_3Si_4O_{10}(OH)_2 \quad \text{(R6)}$$

orthopyroxene + water = serpentine + talc

$$Mg_2SiO_4 + MgSiO_3 + 2H_2O \rightarrow Mg_3Si_2O_5(OH)_4 \quad \text{(R7)}$$

olivine + orthopyroxene + water = serpentine

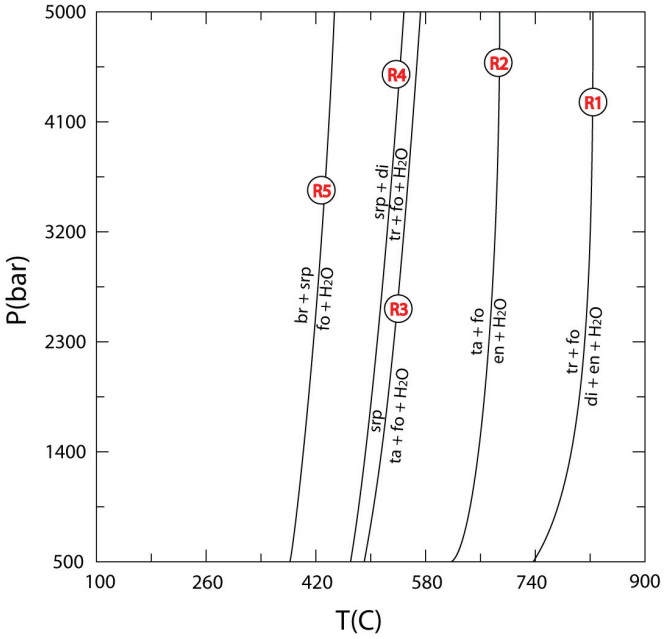

Figure 2. P-T relations between olivine (fo), orthopyroxene (en), clinopyroxene (cpx), tremolite (tr), talc (ta), serpentine (srp) and brucite (br) in the CMSH system. Calculations were done using Perple_X (Connolly and Petrini, 2002) and H_2O was treated as a saturated phase throughout the P-T range.

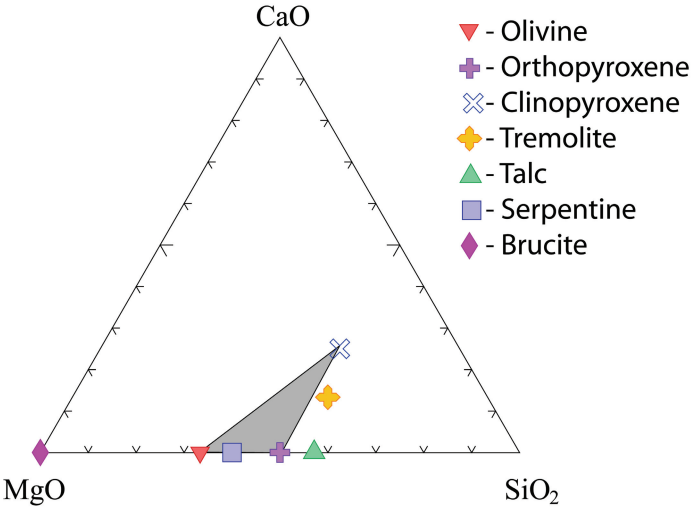

Figure 3. Composition plot of ultramafic minerals and related hydrous products in the CaO-MgO-SiO_2 system. Shaded region shows the compositional range of peridotites and pyroxenites.

1.3 Serpentine textures

Serpentine minerals generally have sub-microscopic grain sizes and can only be identified with the aid of X-ray diffraction or electron microscopy (O'Hanley, 1996). Serpentine textures under the polarizing microscope have been discussed in detail by Wicks and Whittaker (1977) and O'Hanley (1996), and are divided into three categories. Pseudomorphic textures preserve the texture present in the precursor rock while non-pseudomorphic textures do not. Transitional textures preserve some of the textures previously present in the protolith. A brief description of pseudomorphic and non-pseudomorphic textures is given below.

1.3.1 Pseudomorphic textures

Serpentine forms pseudomorphic textures after neso-, ino- and phyllo-silicates. Serpentine pseudomorphs after pyroxenes, amphiboles, talc and mica are known as bastites (Fig. 4A). Bastites preserve the structure of the precursor minerals such as evidence for plastic deformation in enstatite grains. Previous studies using optical microscopy and X-ray diffraction (Wicks and Whittaker, 1977; Wicks and Plant, 1979) have found that the serpentine in pyroxene bastites consists of lizardite *1T* with minor amounts of two-layer lizardite and chrysotile (Le Gleuher et al., 1990). Enstatite is replaced topotactically by serpentine with minor amounts of talc and chlorite when the fluid flow in the system is restricted and the process is diffusion-controlled; whereas in areas of high fluid flux, randomly oriented, fine-grained serpentine and amorphous material replace enstatite (Le Gleuher et al., 1990; Viti et al., 2005).

Pseudomorphic textures of serpentine after olivine are described as mesh or hourglass textures. Mesh textures consist of serpentine in the mesh rim with relict olivine grains or optically distinct serpentine in the mesh cores (Fig. 4B). The outer edge of the mesh rim corresponds to a grain boundary or a fracture within the grain (O'Hanley, 1996). The mesh rim serpentine consists of parallel, apparent fibers perpendicular to the contact between the mesh rim and mesh core. In hourglass textures, the mesh core serpentine is optically indistinguishable from the mesh rim serpentine and is related to fractures rather than grain boundaries (O'Hanley, 1996).

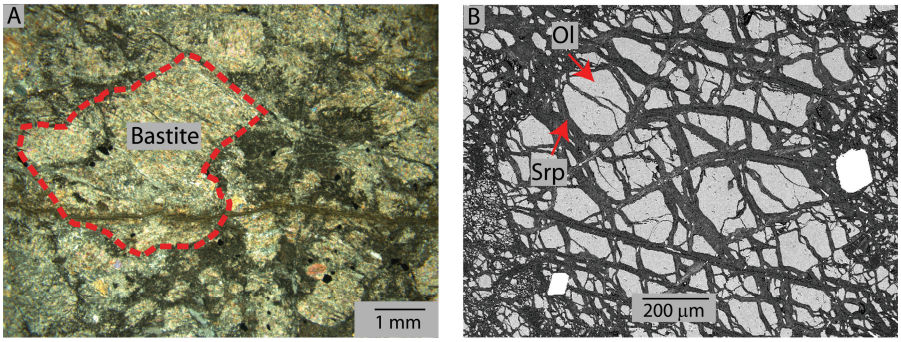

Figure 4.A. Photomicrograph of a bastite formed after orthopyroxene. Talc and serpentine replace the orthopyroxene grain preserving the grain boundaries. B. BSE image of mesh texture in a dunite. Serpentine (Srp) forms at the mesh rims surrounding relict mesh cores of olivine (Ol).

1.3.2 Non-pseudomorphic textures

Non-pseudomorphic textures are divided into interlocking and interpenetrating textures. Serpentine in interpenetrating textures consist of optically distinguishable, elongate blades of antigorite (Fig. 5; O'Hanley, 1996). Interlocking textures consists of equant grains of serpentine and may consist of antigorite, lizardite and/or chrysotile (O'Hanley, 1996).

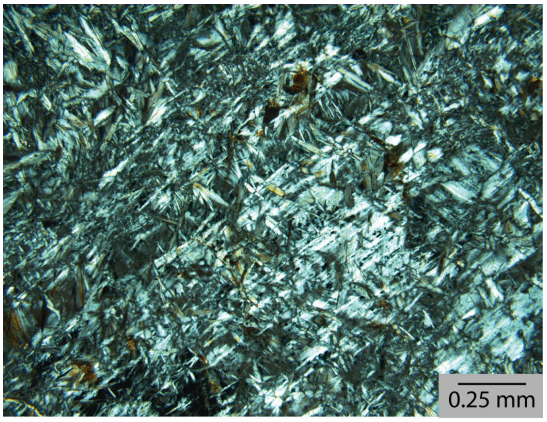

Figure 5. Photomicrograph of non-pseudomorphic interpenetrating texture in serpentinites consisting of optically distinguishable blades of antigorite.

2 Serpentinite settings

Serpentinization is often observed in a variety of tectonic environments and is caused by the hydration of mafic or ultramafic rocks due to interaction with fluids of various origins. The occurrence of serpentinites in the oceans is mainly associated with downward fluid flow along major fault structures which penetrate deep into the oceanic lithosphere. The various settings in which serpentinites occur are briefly outlined below.

2.1 Divergent margins

Serpentinites have been dredged along mid-ocean ridges in places where peridotites have been exposed to seawater. Serpentinization is more pronounced at ultraslow- to slow-spreading centers (e.g. Mid-Atlantic Ridge). Karson et al. (1987) suggested a model which accounts for the effects of magmatism-dominated vs. extension-dominated spreading at slow-spreading, mid-ocean ridges. The mid-ocean ridge will go through phases when extension of the ridge crest is dominated by magmatic activity during phases of magmatic intrusion. Due to an episodic supply of magma, these phases will be interspersed with periods without magmatic activity (MacDonald, 1982; Harper, 1984). Crustal thinning occurs during these periods due to a lack of magma supply resulting in the formation of normal faults and exposure of the deep oceanic lithosphere to seawater. Mével et al. (1991) added that serpentinization of the exposed peridotite may also result in swelling due to the associated bulk volume expansion and enhance relief in the region. Serpentinites are also found at the axial valley walls and floor (Mével, 2003). Megamullions, which are long-lived, low-angled detachment faults, form at slow-spreading ridges and expose large portions of the oceanic lithosphere where serpentinization occurs. In contrast, the continuous supply of magma at fast-spreading ridges (e.g. East Pacific Rise) drives extension and results in high temperatures and a lack of extensive normal faulting inhibiting the serpentinization of rocks near the ridge axis. Serpentinization at fast-spreading ridges can, however, occur off-axis where the temperatures could be within the stability field of serpentine. Serpentinites also occur at transform faults and associated deep-seated fracture zones or at the tips of propagating rifts (e.g. Hess Deep; Fryer, 2002).

Downward fluid flow in the recharge zone of a hydrothermal system located near a spreading axis is largely attributed to the presence of tectonically activated faults and fracture networks (e.g. Schroeder et al., 2002; Mével, 2003). Fracture networks formed due to the injection and subsequent thermal contraction of the surrounding diabases may also result in a percolating structure allowing fluid access to the underlying crust (Lowell and Germanovich, 1994). Another mode of fluid penetration was suggested by Lister (1974) where the hydrothermal system migrates downwards through the crust. He suggested that tensile stresses set up due to the temperature difference between the colder, hydrothermal system and the hotter underlying rock could be sufficient to crack the hot crustal rock and allow downward fluid migration. The cold fluids penetrate through the crust reaching the reaction zone where it is heated due to the proximity of a magma body and water-rock reactions are initiated. The lighter, hot fluids then ascend along faults or fractures to the seafloor and vents into the ocean (Lowell and Germanovich, 1994; Bach et al., 2002).

Cann and Strens (1989) suggest a simple model to describe fluid flow in a hydrothermal system at spreading ridges. Seawater penetrates through the seafloor to form a broad recharge zone of low permeability through Darcy flow, although focused fluid flow may occur along faults or zones of intense jointing within the zone. The fluid subsequently reaches the reaction zone where the temperature of fluid increases towards the base of the reaction zone. The fluid is then expunged through a narrow discharge zone and exits towards the seafloor giving rise to a hydrothermal vent. The pressure distribution in the system, which is the sum of the hydrostatic and frictional resistance components, is the driving force for fluid flow. The difference between the hydrostatic pressure at the base of the recharge zone and the base of the discharge zone (buoyancy pressure) accelerates flow in the system, while frictional resistance would retard fluid flow.

Nicolas et al. (2003) describe a fluid circulation model based on a fossil, high-temperature hydrothermal system in the Oman ophiolite. The system is fed by a recharge zone in the oceanic crust made up of a microcrack network parallel to the paleo-ridge plane. The microcracks in the recharge zone are thought to have developed due to:

1. ridge-related tensile stresses above the brittle-ductile limit.
2. thermal contraction within the gabbros where lithospheric stresses are insufficient.

3. viscous flow at depth in the underlying magma chamber and uppermost mantle.

The fluids flowing through the recharge zone could then trigger hydrous melting in the gabbros. Nicolas et al. (2003) suggest that these pockets of hydrous melt are the sources for the hydrated gabbroic dykes which make up the deeper part of the discharge zone of the system.

2.2 Convergent Margins

Serpentinization of the mantle wedge at active convergent margins could occur due to reaction with fluids released by the subducting slab (Fryer and Fryer, 1987). The forearc region on nonaccretionary convergent margins such as the Puerto Rico, Tonga and Izu-Bonin/Mariana arc systems have been serpentinized by such fluids (Fryer, 2002). The deep trenches associated with some nonaccretionary (e.g. Tonga and Izu-Bonin/Mariana) margins expose the forearc mantle resulting in serpentinization. Serpentine seamounts have been found 50 to 120 km away from the trench axis in the Mariana forearc and are interpreted as diapirs (O'Hanley, 1996). The seamounts are described as <10 to 30 km wide mud volcanoes consisting of serpentinite fragments in a serpentine mud (O'Hanley, 1996). The serpentinite fragments were derived from dunites and harzburgites and are thought to be from the sub-arc mantle. Three models have been proposed to explain the formation of serpentine seamounts in a forearc setting. The first model suggests that serpentinization occurred shortly after the initiation of subduction and the resulting diapirs ascended along fractures in the forearc caused by tectonic erosion (Bloomer, 1983). Fryer et al. (1985) proposed serpentinization was caused by the dehydration of the subducting slab. The resulting diapirs rose through vertical faults in the forearc which were formed by the subduction of seamounts initially oceanward of the trench. The third model proposed by Saleeby (1984) suggests that the serpentine diapirs were formed from mantle rocks beneath or within the fracture zone which initiated subduction.

2.3 Ophiolites

Ophiolites are defined as an assemblage of mafic to ultramafic rocks. It includes an ultramafic complex consisting of dunite, harzburgite and lherzolite commonly with tectonite fabrics at a deeper level. The ultramafic rocks are overlain by a gabbroic complex, a mafic sheeted-dyke complex and a mafic-volcanic complex with pillow

flows towards shallower levels (Penrose Field Conference, 1972). Sedimentary rocks are found at the uppermost levels of an ophiolite complex. Ophiolites are interpreted as to have formed at either fast- or slow-spreading ridges (Pearce et al., 1984; Dick and Bullen, 1984; Boudier and Nicolas, 1985). The generally accepted mechanisms of ophiolite emplacement is thrusting of the forearc mantle over the accretionary wedge in a forearc setting or thrusting over the passive margin or the arc in a back-arc setting (e.g. Laurent, 1980; Harper, 1984; El-Shazly and Coleman, 1990; Cawood and Suhr, 1992; Egal, 1992; Harris, 1992; Wirth and Bird, 1994). Oceanic serpentinites occur in various ophiolites such as the Austro-alpine ophiolites (Früh-Green et al., 1990) in the Alps and the Josephine ophiolite in California (Coulton and Harper, 1992). Calcite replacing serpentine in brecciated veins associated with oceanic fault scarps found in the Alps possesses $\delta^{13}C$ and $\delta^{18}O$ values that are consistent with formation from seawater (Früh-Green et al., 1990). This implies that the pre-existing serpentine must also have been oceanic. Evidence from other ophiolites such as in the Rif Mountains and the Josephine ophiolite also suggest that serpentinization predated thrusting and was oceanic in origin (O'Hanley, 1996). Evidence from the Josephine ophiolite (Harper et al., 1990) and the Trinity peridotite (Peacock, 1987) in California suggests that serpentinization in ophiolites can also occur during thrusting at greenschist facies.

2.4 Greenstone belts

Greenstone belts are Archean to Proterozoic regions comprised of mafic to ultramafic rocks, felsic volcanics and sedimentary rocks. Ultramafic rocks occur as dunite cumulates in komatiitic lava flows or as dunite and pyroxenites in sills (O'Hanley, 1996). Carbonate alteration in the greenstone belts is attributed to seawater alteration and regional metamorphism. The serpentine minerals in some greenstone belts predate the formation of carbonates and stable-isotope data suggest that seawater or a hydrothermal fluid derived from fluid-rock interaction was the cause of serpentinization (Kyser and Kerrich, 1991; O'Hanley et al., 1993).

3 Effects of serpentinization

The hydration of 'dry' peridotites results in the formation of hydrous phases like serpentine and strongly modifies the physical properties of the rock. Some of the major consequences of serpentinization are summarized below.

3.1 Density changes

The average densities of unaltered peridotite and serpentine are approximately 3.3 g/cm^3 and 2.5 g/cm^3 respectively (Mével, 2003). It is evident that serpentinization causes a drastic decrease in density of the affected rocks. Miller and Christensen (1997) have shown that the density of serpentinized rock is inversely proportional to the amount of serpentinization (Fig. 6A). The volume changes occurring during serpentinization is still a subject of debate. It, however, seems that serpentinization of ultramafic rocks is accompanied by very little mobilization of major elements, with the exception of calcium (e.g. Coleman and Keith, 1971; Komor, et al., 1985), which would indeed result in a volume increase in the serpentinized rocks. The increase in volume can be accommodated by tectonic activity in an extensional environment and is evident by vein formation (Mével, 2003). It could also result in the deformation of the serpentinized peridotite. O'Hanley (1992) argued that the volume increase accompanying serpentinization of peridotites results in the formation of cross-fractures present at the boundary between partly and completely serpentinized peridotites forming a 'kernel' pattern at the outcrop scale. The cross-fractures are interpreted as expansion cracks formed in the rim of the kernel due to an increase in volume at the core of the kernel. Evidence for deformation as a result of serpentinization has also been documented in the Leka Ophiolite Complex, Norway (Iyer et al., 2007a, b). The deformation occurs in orthopyroxenite dykes embedded in a dunite matrix. Textural observations and equilibrium thermodynamic calculations indicate that serpentinization of the dunites occurred after the orthopyroxenite dykes had been hydrated. The volume increase associated with serpentinization of dunites results in the orthopyroxenite dykes being effectively squeezed normal to their strike direction. This results in the formation of fractures in the orthopyroxenite dykes which are perpendicular to the dyke-dunite contact irrespective of the strike direction of the dykes. The 2-D fracture networks observed in the orthopyroxenite dykes are

interpreted as hierarchical fracture patterns and are formed as a response to the stress-field generated by the expanding dunite.

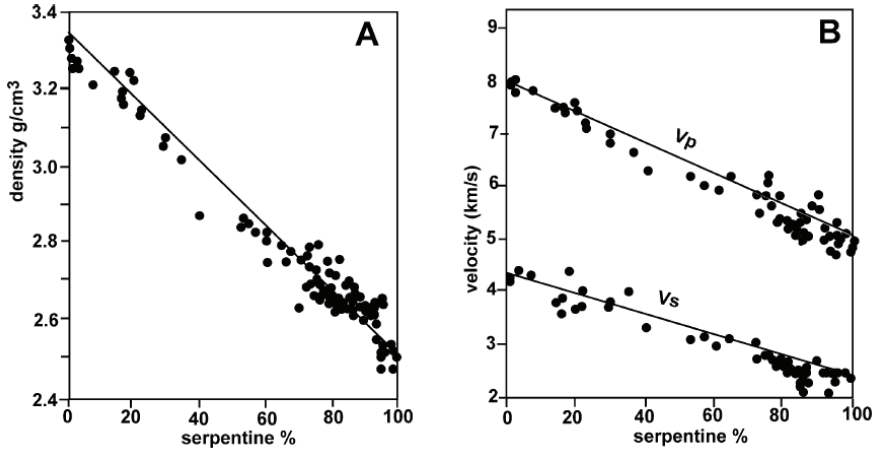

Figure 6. Plot of densities (A) and seismic velocities (B) as a function of degree of serpentinization (From Mével, 2003).

3.2 Seismic velocity

The decrease in density of affected rocks during serpentinization also influences the seismic velocities. Seismic velocities measured on serpentinites show a strong inverse dependence on the amount of serpentinization (Miller and Christensen, 1997; Mével, 2003; Fig. 6B). The replacement of olivine grains by an isotropic network of serpentine results in the decrease of anisotropy of P- and S-waves with increasing serpentinization (Horen et al., 1996). Miller and Christensen (1997) observed that the seismic velocities and densities of partially serpentinized (30-50%) peridotites are indistinguishable from that of gabbroic rocks. The effect of serpentinization on the seismic velocities of the affected rocks may lead to a misinterpretation of the location of the oceanic MOHO (transition between magmatic, mafic rocks and residual, ultramafic rocks) due to the similarities in seismic velocities of gabbro and serpentinized rocks. The seismic front could instead indicate a hydration front or thermal boundary (500°C isotherm) which delineates serpentinized and fresh peridotites (Mével, 2003). The results of Miller and Christensen (1997) are based on the seismic velocities measured in peridotites containing lizardite and chrysotile. However, recent results indicate that antigorite-bearing peridotites may have much

higher seismic velocities than lizardite and chrysotile-bearing peridotites (Watanabe et al., 2007). The compressional wave velocity varies depending on the orientation of antigorite grains in the sample and ranges between 8.4 km/s (parallel to the b-axis of the grain) and 6.6 km/s (perpendicular to the b-axis of the grain).

3.3 Magnetic properties

Serpentinization of ultramafic rocks produces magnetite due to the oxidation of the iron component present in olivine and pyroxenes and therefore strongly affects the magnetic properties of the rock. The magnetic susceptibility and ferromagnetic behavior of peridotites increases with increasing amounts of serpentinization due to production of magnetite (Toft et al., 1990) and is linearly related to the amount of magnetite (Oufi et al., 2002). High degrees of serpentinization also result in an increase in natural remnant magnetization (NRM) which can contribute to oceanic magnetic anomalies (Dyment et al., 1997; Oufi et al., 2002). However, the increase in magnetic susceptibility with the degree of serpentinization is not linear as would be predicted by a single-step reaction of olivine and water to serpentine, brucite, magnetite and hydrogen (Fig. 7; Bach et al., 2006). Initial serpentinization (<60-70%) partitions iron obtained from the breakdown of olivine and orthopyroxene into iron-rich serpentine (up to 6% FeO) and brucite resulting in modest magnetite contents (Oufi et al., 2002; Bach et al., 2006). The production of magnetite is later accelerated (>60-75% serpentinization) due to the destabilization of Fe-rich serpentine and brucite, and formation of iron-poor serpentine and brucite (2-3% FeO; Oufi et al., 2002; Bach et al., 2006). In some environments, the breakdown of orthopyroxene, during the later stages of serpentine, strongly affects the composition of the reacting fluid (Bach et al., 2006). The high silica activities results in the breakdown of ferroan brucite to form serpentine and magnetite. These models contain two-steps which includes the initial formation of Fe-rich serpentine and brucite form olivine and pyroxene. The Fe-rich hydrous phases break down at later stages to form Fe-poor serpentine and brucite in addition to magnetite. This two-step model has been proposed to explain the exponential magnetic susceptibility curve observed in serpentinized peridotites (Fig. 7). Oufi et al. (2002) also show that the NRM of serpentinized peridotites can be as high as basalts due to the presence of small magnetite grains associated with mesh-textured serpentine. However, low-

temperature oxidative alteration partially alters magnetite to maghemite resulting in lower NRM and magnetic susceptibilities.

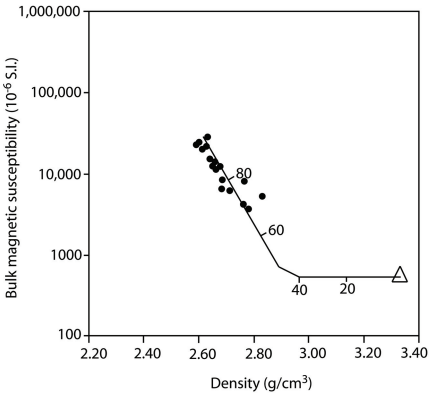

Figure 7. Plot of bulk magnetic susceptibility and density for whole rock samples of serpentinized peridotites (dark circles; 70-100% serpentinized). The triangle represents a typical fresh peridotite. The solid trend line represents the results for the two-step model. Marks and labels on the trend line refer to the Mol% of serpentine formed in the first step. (Modified after Bach et al., 2006).

3.4 Rheology

Serpentinization of peridotites changes the rheology of the altered rocks and can have important implications for tectonic activity occurring within the oceanic lithosphere. The presence of small amounts of serpentine (~10%) significantly reduces the strength of an altered peridotite and is similar to that of pure serpentine (Escartín et al., 1997a, b; Escartín et al., 2001). The deformation is primarily accommodated by nondilatant brittle deformation of serpentine present in the peridotite while olivine remains undeformed (Escartín et al., 2001). A transition from brittle (localized) to ductile (distributed) deformation occurs as the confining pressure increase from ~200 to ~400 MPa and corresponds to change in deformation mechanism from brittle faulting to cataclastic flow (Escartín et al., 1997a). Deformation in both regimes is accommodated by shear microcracks. In the brittle regime, the strain localizes on a single fault formed at high angles (30-45°) to the shortening direction while in the ductile regime, numerous shear zones that are homogeneously distributed throughout the sample accommodate small amounts of strain (Escartín et al; 1997a). The low internal friction coefficient of serpentine (μ_i~0.3) can significantly reduce the optimal fault angle of large-displacement faults and increase the displacement along low-angle

detachment faults providing paths for fluid infiltration at the end segments of slow-spreading ridges (Escartín et al; 1997b). Formation of serpentine along these fault planes would also enhance strain localization (Escartín et al; 1997b; Escartín et al; 2001). The changes in rheology accompanying serpentinization can thus influence the tectonics of the oceanic lithosphere due to weakening and promote formation of fault structures and strain localization within them.

4 Ultramafic-hosted hydrothermal systems

Hydrothermal systems have been discovered in basalt- and ultramafic-hosted systems along mid-ocean ridges. Some examples of ultramafic-hosted hydrothermal systems along the Mid-Atlantic Ridge have been found at 30°N (Lost City), 36°14´N (Rainbow) and 14°45´N (Logatchev).

The permeation of water down into the serpentinite basement of the system may occur due to tectonic activity, the presence of long-lived detachment faults at slow-spreading ridges, isostatic uplift and exfoliation induced by mass wasting (Kelley et al., 2001). The heat required to drive the hydrothermal systems may be obtained (i) from crystallizing basaltic magmatic intrusions, (ii) from the lithospheric mantle, and (iii) exothermic (serpentinization) water-rock reactions (Fyfe and Lonsdale; 1981; Bach, et al., 2002; Mével, 2003).

Vent fluid temperatures for ultramafic-hosted hydrothermal systems range between ~40° (Lost City) and 365°C (Rainbow and Logatchev). Lowell and Rona (2002) showed that, in the absence of an external heat source, hydrothermal temperatures of above 100°C can be achieved when serpentinization rates are very high (10^3 kg/s) and mass flow rates are low (10 kg/s). However, based on experimental diffusion rates, serpentinization rates are extremely low (0.1 kg/s; MacDonald and Fyfe, 1985) and cannot be the only source of heat in high-temperature hydrothermal systems (Rainbow and Logatchev). Recent studies have however shown that the volume changes accompanying serpentinization may induce fracturing in the affected ultramafic rocks (e.g. O'Hanley, 1992; Iyer et al., 2007a, b). Serpentinization would generate permeability in the rock and therefore the rate of serpentinization may be higher than predicted from a pure diffusion model. In addition, the high flow rates (500 kg/s) of the vent fluids (Thurnherr and Richards, 2001; Bach et al., 2002; Douville et al., 2002), the high temperatures of the vent fluids (>364°C) and the on-axis location of the Rainbow hydrothermal field suggest that the heat source is magmatic (Allen and Seyfried; 2004).

The temperature of vent fluids emanating from the Lost City hydrothermal field is relatively cool (40-75°C). On the basis of the isotopic compositions of vent fluids, Kelley et al. (2001) argued that the heat derived from serpentinization reactions occurring due to the reaction of mantle peridotite with seawater is sufficient to drive

the hydrothermal system and produce vent fluid temperatures up to 91°C. However, theoretical calculations to reproduce the fluid chemical composition combined with heat balance models suggest that the heat source of the Lost City hydrothermal vent field may be due to the proximity of magma body or to the deep penetration of fluids along long-lived faults (Allen and Seyfried, 2004). Allen and Seyfried (2004) use a heat balance calculation to account for the temperature rise contributed by the exothermic reaction of olivine to serpentine:

$$\Delta T = \frac{\Delta H}{\left(\frac{W}{R\lambda} C_w + C_r\right)}$$

where

ΔT = temperature rise due to the exothermic reaction

ΔH = enthalpy change of the reaction

W = fluid mass flow rate

R = reaction rate

λ = olivine to serpentine conversion

C_w = heat capacity of water

C_r = heat capacity of the rock

W/R, in the above equation, indicates the total mass of fluid involved in the serpentinization of a mass of peridotite in a given amount of time. Existing data suggests that the value for *W/R* is 1 for high-temperature serpentinites and significantly higher for low-temperature serpentinites (Agrinier and Cannat, 1997; Bonatti et al., 1984). Values for λ range between 0 and 1; where 1 represents complete conversion of olivine to serpentine and lower values imply fractionally less olivine to serpentine conversion. Assuming complete serpentinization (λ=1), Allen and Seyfried (2004) found that the heat generated during serpentinization reaches a maximum value of approximately 50°C for *W/R* ratios of 1 and higher values of *W/R* results in lower amounts of heat generation (see Fig. 4 from Allen and Seyfried, 2004). Using the temperature dependence of olivine reaction rate data (λ values*)* from Martin and Fyfe (1970) and a *W/R* ratio of 1, they found that the temperature change due to serpentinization describes a bell-shaped curve with a maximum temperature change of 50°C occurring at an initial temperature of 270°C which corresponds to the optimal

temperature for olivine serpentinization. Allen and Seyfried (2004) present additional arguments for the presence of a non-exothermic source of heat:

1. The hydrolysis of olivine to serpentine is sluggish at the measured temperatures of the Lost City vent fluids (40-75°C).
2. Assuming that ambient seawater is the fluid source, heat generation from exothermic mineral reactions would require extremely low fluid-rock mass ratios to attain the measured vent fluid temperatures. This would also result in high concentrations of dissolved Cl, K and Na due to removal of water during serpentinization which is not observed at Lost City.
3. Geochemical modeling requires vent fluid temperatures between 150°-250°C to account for the measured dissolved Ca and SO_4 concentrations in the Lost City vent fluids.
4. Conductive cooling of the fluid during transit from the alteration site to the seafloor could explain the relatively low vent fluid temperature and subsequent seawater mixing with the fluid may result in the observed calcite and brucite chimney formations.

Alt and Shanks (2003) alternatively argue that the vent fluids at Lost City are a result of the interaction of a seawater-derived fluid with off-axis gabbroic intrusions.

The composition of vent fluids in ultramafic-hosted hydrothermal systems largely depends on the seawater-peridotite reactions and water-rock ratios. Experimental results suggest that vent fluids issuing from ultramafic-hosted hydrothermal systems at low water-rock ratios should have lower Si, Mn, Fe, Al and K; a higher pH; and much higher H_2 and CH_4 values relative to basalt-hosted hydrothermal systems at similar temperatures (Wetzel and Shock, 2000; Tivey, 2007). However, vent fluid compositions measured at the Rainbow and Logatchev hydrothermal fields are acidic and contain high concentrations of Fe and Mn, specifically fluids from the Rainbow field (see Table 1). As described above, the temperatures of vent fluids at these sites are also considerably higher. Experiments by Allen and Seyfried (2003) have show that orthopyroxene is readily altered in the presence of water at temperatures equal to or greater than 400°C, 500 bars; while olivine hydrolysis is sluggish at these high temperatures. The dissolution of pyroxene minerals at high temperatures results in high dissolved concentrations of SiO_2, Ca, and H_2. The high SiO_2 concentrations stabilize talc and tremolite resulting in low pH values (Allen and Seyfried, 2003). The high temperature coupled with low pH enhances magnetite solubility resulting in

relatively high dissolved Fe concentrations in the fluid when compared to seawater-basalt reactions (Allen and Seyfried, 2003; Tivey, 2007). Fe/Mn ratios increase as a consequence of the increasing stability of Fe-Cl complexes with increasing temperatures and decreasing pH (Douville et al., 2002). The high temperatures of the Rainbow vent fluids also inhibit the precipitation of Fe and Cu minerals during upflow (Douville et al; 2002). The vent fluid composition of the Rainbow hydrothermal system may therefore be a consequence of the high temperatures at which olivine hydrolysis is slow and pyroxene dissolution controls the evolution of the reacting fluid.

Vent fluids associated with the hydrothermal alteration of peridotites contain high concentrations of H_2 and CH_4 due to the resulting reducing conditions during serpentinization and are of an order of magnitude higher than the contents present in vent fluids in basaltic-hosted hydrothermal systems (Charlou et al., 2002). Metals present in ultramafic rocks undergo redox reactions and hydrogen is released during the thermal dissociation of water (French, 1966). Hydrogen is also produced from the breakdown of ferrous hydroxide (iron component in brucite) during serpentinization (Moody, 1976; Neal and Stanger, 1983; Charlou et al., 2002). The oxidation of Fe^{2+} and subsequent production of H_2 during the serpentinization of olivine is given by Moody (1976):

$$5Mg_2SiO_4 + Fe_2SiO_4 + 9H_2O \rightarrow 3Mg_3Si_2O_5(OH)_4 + Mg(OH)_2 + 2Fe(OH)_2 \quad \text{(R8)}$$

forsterite + fayalite + water = serpentine + brucite + ferroan brucite

$$3Fe(OH)_2 \rightarrow Fe_3O_4 + H_2 + 2H_2O \quad \text{(R9)}$$

ferroan brucite = magnetite + hydrogen + water

Methane produced during serpentinization is attributed to Fischer-Tropsch type reactions. Fischer-Tropsch synthesis is an industrial process whereby CO_2 reacts with hydrogen forming hydrocarbon gas (R10; Berndt et al., 1996):

$$CO_2 + 4H_2 \rightarrow CH_4 + 2H_2O \quad \text{(R10)}$$

carbon dioxide + hydrogen = methane + water

During serpentinization experiments conducted by Berndt et al. (1996) at 300°C and 500 bars, it was observed that magnetite can act as a catalyst for the methanogenesis process as it effectively lowers the activation energy of Fischer-Tropsch reactions. Higher hydrocarbons like ethane and methane are also produced during the Fischer-Tropsch reactions. Field and experimental results, therefore, imply that serpentinization of ultramafic rocks plays an important role in the formation of abiogenic hydrocarbons. This may also significantly contribute to the formation of methane seeps associated with ultramafic rocks (e.g. Coveney et al; 1987; Abrajano et al, 1988, 1990; Rona et al., 1992; Sherwood-Lollar et al., 1993; Charlou and Donval; 1993) and methane gas hydrates (Haggerty, 1991).

	Logatchev	**Rainbow**	**Lost City**	**TAG**	**Seawater**
Host rock	Peridotite	Peridotite	Peridotite	Basalt	
Temperature °C	352	365	40-75	363	2
pH	3.3	2.8	9.0-9.8	3.1	7.8
Si mM	8.2	6.9	-	20	<0.2
Al µM	4.0	2.0	-	10	<0.1
Fe µM	2500	24050	-	5170	0.0045
Mn µM	330	2250	-	710	0.0013
K mM	21.9	20.4	-	18	9.8
CH_4 mM	2.1	2.5	0.13-0.28	0.15-0.16	x4 x 10^{-7}
H_2 mM	12.0	16	0.25-0.43	0.18-0.23	x4 x 10^{-4}
References	Charlou et al., 2002; Douville et al., 2002	Charlou et al., 2002; Douville et al., 2002	Kelley et al., 2001	Charlou et al., 1996; Douville et al., 2002	

Table 1. Comparison table of vent fluid chemistry from various hydrothermal fields and seawater.

5 Serpentinization and implications for life

Serpentinization of ultramafic rocks and subsequent Fischer-Tropsch reactions result in the production of significant quantities of hydrogen, methane and lower quantities of long-chain hydrocarbons (16-29 carbon atoms; Holm and Charlou, 2001; Charlou et al., 2002). Hydrogen produced during serpentinization is used by lithoautotrophs (organism using an inorganic substrate to obtain inorganic electrons) for biosynthesis at low temperatures (Holm and Charlou, 2001; Kelley et al., 2005). At higher temperatures, the availability of abiotic organic compounds can sustain organotrophic organisms (energy derived from organic sources) (Holm and Charlou, 2001). Kelley et al. (2001) found extensive microbial biofilm production linked to the Lost City hydrothermal field. In addition, a number of small invertebrates like snails, bivalves, polychaetes, amphipods and ostracods have been found in association with the active carbonate chimney structures present at Lost City (Boetius, 2005; Kelley et al., 2005). The large quantities of ultramafic rocks present during the Archean age of the Earth and the discovery of Fischer-Tropsch type reactions in ultramafic hydrothermal systems may have provided a suitable environment to sustain life (Holm and Charlou, 2001).

6 Authorship statement and summary of papers

The thesis is presented as a collection of three scientific papers dealing with the chemical and mechanical feedbacks accompanying hydration processes in ultramafic rocks.

In the first article, I was responsible for sample collection and chemical analysis, except for the bulk rock chemical analysis which was carried out at Royal Holloway, University of London. In addition, I initiated and wrote the paper. I also carried out equilibrium thermodynamic calculations using Perple_X, interpretation of petrological textures and mineral reactions. Bjørn Jamtveit, Håkon Austrheim and Timm John contributed by way of discussions and proof-reading. Bjørn Jamtveit and Håkon Austrheim were also part of several field excursions.

In the second article, I was responsible for the collection of field data which included fracture spacing and layer thickness data of the orthopyroxenite dykes. I wrote MATLAB routines for image analysis of fracture patterns. I also wrote a 2-D Finite Element Method code which was used in the development of the paper. I and Joachim Mathiesen jointly developed the fragmentation model. All the co-authors contributed to the paper through discussions. Bjørn Jamtveit assisted me in writing the paper. Anders Malthe-Sørenssen and Jens Feder supervised the development of image analysis routines.

In the third manuscript, I developed a 1-D Finite difference model of an extending layer with frictional interfaces in addition to writing the paper. Yuri Podladchikov contributed by way of supervision, discussions and proof-reading.

The papers are arranged in a logical sequence which ties together the observations and results obtained through the duration of the Ph.D. The first paper deals with the petrological and chemical effects associated with the hydration of ultramafic rocks in the Leka Ophiolite Complex. Although, major elements present in the ultramafic rocks do not seem to be mobile on the regional scale during hydration, textural evidence shows that Fe, Mn and Ca can be transported along grain-scale distances and play an important role in the formation of metamorphic minerals. Textural observations and equilibrium thermodynamic calculations help constrain the sequence of phase transitions through the evolution of the ultramafic rocks during hydration. An important outcome of the serpentinization reactions is the volume change

occurring in the affected rocks which may cause deformation. A key observation is that the major volume changes taking place in the dunites occur after the hydration of the orthopyroxenite dykes, i.e. at lower temperatures. The second paper deals with the fracturing of the orthopyroxenite dykes as a response to the stresses set up during the expansion of the dunites. The fracture patterns in the dykes have been statistically characterized as hierarchical patterns which are dominated by four-sided polygons. The fractures in such patterns develop sequentially and later fractures develop orthogonally to earlier fractures. A fragmentation model was also developed to provide insight into the number of generations of fractures in the observed patterns and the initial fracture lengths. An important observation is that the thickness of the orthopyroxenite dykes controls the density of fractures in the dyke. A 2-D FEM model was developed to study the effect of layer thickness on the fracture spacing within a layer with perfectly welded interfaces. The model shows that there exists a critical fracture spacing to layer thickness ratio (0.8-1.0) below which the horizontal stress component turns compressive, i.e. no tensile fractures can form. However, field data shows that the fracture spacing to layer thickness ratios in the orthopyroxenite dykes are below the critical value with the mean value of 0.45±0.2. The third paper investigates the effect of friction along the dyke-dunite interface on the fracture spacing to layer thickness ratios. Results from a 1-D FDM model of a layer with frictional interfaces shows that the minimum fracture spacing to layer thickness ratio is directly dependent on the ratio of the tensile and shear strength of the material. The ratios obtained for a layer with frictional interfaces can be as low as 0.10 and are in agreement with field observations.

6.1 Paper I (Serpentinization of the oceanic lithosphere and some geochemical consequences: Insights from the Leka Ophiolite Complex, Norway)

In this paper, we focus on the chemical and petrophysical evolution of the ultramafic rocks of the Leka Ophiolite Complex (LOC) through the serpentinization process. The LOC provides a fossil record of the ocean-floor serpentinization over a wide range of temperatures. Equilibrium thermodynamic calculations indicate that the hydration process may have been initiated at temperatures as high as 800°C. Detailed petrographical analysis further constrains the upper temperature limit to a minimum of 500-650°C. The reactions and phase changes occurring during serpentinization is

not only dependent on the temperature but also on fluid composition and availability, and the oxidation state of the system.

Although elements like Mg, Si and Al seem to be redistributed within the system during serpentinization at the outcrop scale, there is evidence for grain- and regional-scale transport of elements like Fe, Mn, Ca and Na. Iron and manganese redistribution during the breakdown of primary orthopyroxene and olivine significantly controls the chemistry of metamorphic olivine. Metamorphic olivine in the ultramafic rocks has a wide range of compositions and can have Mg# as low 0.68 and Mn contents as high as 1.5 wt%. The amount of manganese and iron present in metamorphic olivine is also controlled by the oxidation state and fluid flux within the system. The hydration of olivine results in iron- and manganese-rich brucite which when oxidized results in the formation of magnetite and a loss of manganese. Calcium releasing and consuming reactions occur during serpentinization and contribute to formation of secondary phases. Primary clinopyroxene in the ultramafic rocks acts as a source of calcium while amphiboles and secondary diopsidic clinopyroxene replacing olivine, primary clinopyroxene and orthopyroxene acts as a sink for calcium. Transport of calcium is also evident from the rodingitization of the lower crustal section of the ophiolite suite.

A further consequence of serpentinization is the drastic volume changes which results in deformation of the surrounding rocks. Equilibrium thermodynamics and experimental work (Pawley, 1998; Allen and Seyfried, 2003; Melekhova et al., 2006) show that the alteration of orthopyroxene occurs at higher temperatures where olivine reacts sluggishly. The volume changes occurring at lower temperatures are therefore controlled by the serpentinization of dunites (ΔV~25%) in which the orthopyroxenite dykes are embedded. This leads to the deformation of the orthopyroxenite dykes and subsequent fracturing.

Serpentinization is, therefore, an important process which significantly modifies the chemical and physical properties of rocks, and contributes to metasomatism and deformation in the affected rocks.

6.2 Paper II (Reaction-assisted hierarchical fracturing during serpentinization)

In this paper, we discuss the Mode-I fracture patterns formed in the orthopyroxenite dykes as a result of expansion of the surrounding dunites during serpentinization. The fractures present in the orthopyroxenite dykes are oriented sub-parallel to each other and are perpendicular to the contact between the dunites and the dykes. A quasi 2-D

cross-section through the orthopyroxenite dykes reveals a network of crisscrossing fractures that break the rock up into small domains. The process of fracturing is hierarchical; the initial fracture(s) controls the formation of later fractures where the latter meet the former at right angles and the process is a result of the stress generated due to volume changes and material properties. Statistical analysis on the fracture pattern yields typical characteristics of hierarchical fracture patterns such as the dominance of 4-sided domains and angles of 90° and 180° at fracture junctions (T-junctions). Analysis of domain orientations within the fracture patterns indicate that the stress field induced by the expanding dunite may have been anisotropic leading to a preferential direction for fracture propagation. The scaling behavior of fracture lengths obtained from the 2-D cross-sections range between a power-law and log-normal scaling and exhibit a cross-over at lengths close to the thickness of the orthopyroxenite dyke (sample LE69). A fragmentation model was developed to fit the observed data and predict the initial fracture size and number of fracture generations for a given system. A 2-D linear, elastic FEM model was developed to study the stress regime in a layer with welded interfaces under extension. We find that, for any given strain, the horizontal stress component in the middle of the domain changes from tensile to compressive below a critical fracture spacing to layer thickness ratio of approximately 1.0 and will inhibit the propagation of a Mode-I fracture through the layer. The critical ratio is also observed in the cross-over scaling behavior of the 2-D fracture patterns. The fracture patterns studied in this work indicate that the process of serpentinization resulted in the slow build-up of stresses in the orthopyroxenite dykes which then fractured as a response to the stress field. The dykes preserve a fossil record of the stress-field generated during serpentinization and the fractures further enhance the process of serpentinization by acting as conduits for fluid migration.

6.3 Paper III (Joint spacing driven by differential volume expansion: The role of frictional sliding)

This paper deals with the effect of frictional sliding of the orthopyroxenite dyke along the interface with the surrounding dunites on the fracture spacing to layer thickness ratios observed in the dykes. Field data of fracture spacing in the orthopyroxenite dykes (583 sample points) shows a linear correlation to the dyke thickness and the fracture spacing to layer thickness ratios range between 0.1 and 1.0 with a mean value of 0.45 ± 0.2. The large strain generated by the volume increase in the surrounding

dunites cannot be accommodated by Mode-I fracturing in the orthopyroxenite dykes and some of the deformation has to be inelastic. The inelastic deformation is accommodated by the decoupling and frictional sliding of the orthopyroxenite dyke along the interface. A 1-D Finite Difference Method model of a layer with a frictional interface is constructed to investigate the fracture spacing to layer thickness ratio driven by volume increase in the surrounding matrix. Fractures are allowed to develop in the model if the tensile strength of the material is reached and the layer is decoupled at the interface if the shear stress exceeds the shear strength of the material. The maximum allowed shear stress in the deforming layer is limited by shear strength values obtained from experimental results and has values 3 to 5 times greater than the tensile strength of the layer. We find that the minimum fracture spacing to layer thickness ratio has a one-to-one dependence on the ratio of tensile to shear strength for the materials. Results obtained for runs using the experimentally obtained values for tensile and shear strength results in a minimum fracture spacing to layer thickness of 0.2 which is considerably lower than the ratio predicted by models using a welded interface. Thus, frictional sliding may provide an important control on the fracture spacing in layered rocks.

7 References

Abrajano, T. A., Sturchio, N. C., Bohlke, J. K., Lyon, G. L., Poreda, R. J. and Stevens, C. M., 1988. Methane Hydrogen Gas Seeps, Zambales Ophiolite, Philippines - Deep or Shallow Origin. *Chemical Geology*, **71**, 211-222.

Abrajano, T. A., Sturchio, N. C., Kennedy, B. M., Lyon, G. L., Muehlenbachs, K. and Bohlke, J. K., 1990. Geochemistry of Reduced Gas Related to Serpentinization of the Zambales Ophiolite, Philippines. *Applied Geochemistry*, **5**, 625-630.

Agrinier, P. and Cannat, M., 1997. Oxygen isotope constraints on serpentinization processes in ultramafic rocks from the Mid-Atlantic Ridge (23°N). *Proceedings of the Ocean Drilling Program, Scientific Results, College Station, TX*, **153**, 381-388.

Allen, D. E. and Seyfried, W. E., 2003. Compositional controls on vent fluids from ultramafic-hosted hydrothermal systems at mid-ocean ridges: An experimental study at 400°C, 500 bars. *Geochimica Et Cosmochimica Acta*, **67**, 1531-1542.

Allen, D. E. and Seyfried, W. E., 2004. Serpentinization and heat generation: Constraints from Lost City and rainbow hydrothermal systems. *Geochimica Et Cosmochimica Acta*, **68**, 1347-1354.

Alt, J. C. and Shanks, W. C., 2003. Serpentinization of abyssal peridotites from the MARK area, Mid-Atlantic Ridge: Sulfur geochemistry and reaction modeling. *Geochimica Et Cosmochimica Acta*, **67**, 641-653.

Bailey, S. W., 1988. Structures and compositions of other trioctahedral 1:1 phyllosilicates. *In: Hydrous phyllosilicates other than micas. Bailey, S W. (ed.). Reviews in Mineralogy*, **19**, 169-188.

Bach, W., Paulick, H., Garrido, C. J., Ildefonse, B., Meurer, W. P. and Humphris, S. E., 2006. Unraveling the sequence of serpentinization reactions: petrography, mineral chemistry, and petrophysics of serpentinites from MAR 15°N (ODP Leg 209, Site 1274). *Geophysical Research Letters*, **33**, doi: 10.1029/2006GL025681.

Bach, W., Banerjee, N. R., Dick, H. J. B. and Baker, E. T., 2002. Discovery of ancient and active hydrothermal systems along the ultra-slow spreading

Southwest Indian Ridge 10 °-16°E. *Geochemistry Geophysics Geosystems*, **3**, doi: 10.1029/2001GC000279.

Berndt, M. E., Allen, D. E. and Seyfried, W. E., 1996. Reduction of CO_2 during serpentinization of olivine at 300°C and 500 bars. *Geology*, **24**, 671-671.

Bloomer, S. H., 1983. Distribution and Origin of Igneous Rocks from the Landward Slopes of the Mariana Trench - Implications for Its Structure and Evolution. *Journal of Geophysical Research*, **88**, 7411-7428.

Boetius, A., 2005. Lost City Life. *Science*, **307**, 1420-1422.

Bonatti, E., Lawrence, J. R. and Morandi, N., 1984. Serpentinization of oceanic peridotites: Temperature dependence of mineralogy and boron content. *Earth and Planetary Science Letters*, **70**, 88-94.

Boudier, F. and Nicolas, A., 1985. Harzburgite and Lherzolite Subtypes in Ophiolitic and Oceanic Environments. *Earth and Planetary Science Letters*, **76**, 84-92.

Cann, J. R. and Strens M. R., 1989. Modeling Periodic Megaplume Emission by Black Smoker Systems. *Journal of Geophysical Research-Solid Earth and Planets,* **94**, 12227-12237.

Cawood, P. A. and Suhr, G., 1992. Generation and Obduction of Ophiolites - Constraints from the Bay of Islands Complex, Western Newfoundland. *Tectonics*, **11**, 884-897.

Charlou, J. L. and Donval, J. P., 1993. Hydrothermal Methane Venting between 12°N and 26°N Along the Mid-Atlantic Ridge. *Journal of Geophysical Research-Solid Earth*, **98**, 9625-9642.

Charlou, J. L., Donval, J. P., Fouquet, Y., Jean-Baptiste, P. and Holm, N., 2002. Geochemistry of high H_2 and CH_4 vent fluids issuing from ultramafic rocks at the Rainbow hydrothermal field (36°14′N, MAR). *Chemical Geology*, **191**, 345-359.

Charlou, J. L., Donval, J. P., JeanBaptiste, P. and Dapoigny, A., 1996. Gases and helium isotopes in high temperature solutions sampled before and after ODP Leg 158 drilling at TAG hydrothermal field (26°N, MAR). *Geophysical Research Letters*, **23**, 3491-3494.

Coleman, R. G. and Keith, T. E., 1971. Chemical Study of Serpentinization - Burro Mountain, California. *Journal of Petrology*, **12**, 311-328.

Connolly, J. A. D. and Petrini, K., 2002. An automated strategy for calculation of phase diagram sections and retrieval of rock properties as a function of physical conditions. *Journal of Metamorphic Geology*, **20**, 697-708.

Coulton, A. J. and Harper, G. D., 1992. Timing of serpentinization in the Josephine ophiolite: implications for the oceanic Moho. *EOS, Transactions American Geophysical Union*, **73**, No. 43, 537.

Coveney, R. M., Goebel, E. D., Zeller, E. J., Dreschoff, G. A. M. and Angino, E. E., 1987. Serpentinization and the origin of hydrogen gas in Kansas. *AAPG Bulletin*, **71**, 39-48.

Dick, H. J. B. and Bullen, T., 1984. Chromian Spinel as a Petrogenetic Indicator in Abyssal and Alpine-Type Peridotites and Spatially Associated Lavas. *Contributions to Mineralogy and Petrology*, **86**, 54-76.

Douville, E., Charlou, J. L., Oelkers, E. H., Bienvenu, P., Colon, C. F. J., Donval, J. P., Fouquet, Y., Prieur, D. and Appriou, P., 2002. The rainbow vent fluids (36°14´N, MAR): the influence of ultramafic rocks and phase separation on trace metal content in Mid-Atlantic Ridge hydrothermal fluids. *Chemical Geology*, **184**, 37-48.

Dyment, J., Arkani-Hamed, J. and Ghods, A., 1997. Contribution of serpentinized ultramafics to marine magnetic anomalies at slow and intermediate spreading centres: insights from the shape of the anomalies. *Geophysics Journal International*, **129**, 691-701.

Egal, E., 1992. Structures and Tectonic Evolution of the External Zone of Alpine Corsica. *Journal of Structural Geology*, **14**, 1215-1228.

El-Shazly, A. K. and Coleman, R. G., 1990. Metamorphism in the Oman mountains in relation to the Semail ophiolite emplacement. *In: Robertson, A. H. F., Searle, M. P. and Ries, A. C. (eds.). The geology and tectonics of the Oman region, Geological Society of London, Special Publication*, **49**, 473-493.

Escartín, J., Hirth, G. and Evans, B., 1997a. Nondilatant brittle deformation of serpentinites: Implications for Mohr-Coulomb theory and the strength of faults. *Journal of Geophysical Research*, **102**, 2897-2913.

Escartín, J., Hirth, G. and Evans, B., 1997b. Effects of serpentinization on the lithospheric strength and the style of normal faulting at slow-spreading ridges. *Earth and Planetary Science Letters*, **151**, 181-189.

Escartín, J., Hirth, G. and Evans, B., 2001. Strength of slightly serpentinized peridotites: Implications for the tectonics of oceanic lithosphere. *Geology*, **29**, 1023-1026.

Evans, B. W., Johannes, W., Oterdam, H. and Trommsdorff, V., 1976. Stability of chrysotile and antigorite in the serpentinite multisystem. *Schweizerische Mineralogische und Petrographische Mitteilungen*, **56**, 79-93.

French, B. M., 1966. Some Geological Implications of Equilibrium between Graphite and a C-H-O Gas Phase at High Temperatures and Pressures. *Reviews of Geophysics*, **4**, 223-253.

Früh-Green, G. L., Weissert, H. and Bernoulli, D., 1990. A Multiple Fluid History Recorded in Alpine Ophiolites. *Journal of the Geological Society*, **147**, 959-970.

Fryer, P., 2002. Recent studies of serpentinite occurrences in the oceans: Mantle-ocean interactions in the plate tectonic cycle. *Chemie Der Erde-Geochemistry*, **62**, 257-302.

Fryer, P., Ambos, E. L. and Hussong, D. M., 1985. Origin and Emplacement of Mariana Fore-Arc Seamounts. *Geology*, **13**, 774-777.

Fryer, P. and Fryer, G. J., 1987. Origins of non-volcanic seamounts in forearc environments. *In: Keating, B. H., Fryer, P., Batiza, R., Boehlert, G. W. (eds.). Seamount Islands and Atolls, Geophysical Monograph, American Geophysical Union*, *Washington D.C.*, **43**, 61-69.

Fyfe, W. S. and Lonsdale, P., 1981. Ocean floor hydrothermal activity. *In: Emiliani, C. (ed.). The Sea, 7, Wiley and Sons, New York*, 589-638.

Guggenheim, S. and Eggleton, R. A., 1988. Crystal chemistry, classification, and identification of modulated layer silicates. *In: Bailey, S. W. (ed.). Hydrous phyllosilicates exclusive of micas, Reviews in Mineralogy*, **19**, 675-725.

Haggerty, J. A., 1991. Evidence from Fluid Seeps atop Serpentine Seamounts in the Mariana Fore-Arc – Clues for Emplacement of the Seamounts and Their Relationship to Fore-Arc Tectonics. *Marine Geology*, **102**, 293-309.

Harper, G. D., 1984. The Josephine Ophiolite, Northwestern California. *Geological Society of America Bulletin*, **95**, 1009-1026.

Harper, G. D., Grady, K. and Wakabayashi, J., 1990. A structural study of a metamorphic sole beneath the Josephine ophiolite, western Klamath terrane,

California-Oregon. *Geological Society of America Special Paper*, **255**, 379-396.

Harris, R. A., 1992. Peri-collisional extension and the formation of Oman-type ophiolites in the Banda arc and Brooks Range. *In: Parson, L. M., Murton, B. J. and Browning, P. (eds.). Ophiolites and their modern oceanic analogues, Geological Society of London, Special Publication*, **60**, 301-325.

Holm, N. G. and Charlou, J. L., 2001. Initial indications of abiotic formation of hydrocarbons in the Rainbow ultramafic hydrothermal system, Mid-Atlantic Ridge. *Earth and Planetary Science Letters*, **191**, 1-8.

Horen, H., Zamora, M. and Dubuisson, G., 1996. Seismic wave velocities and anisotropy in serpentinized peridotites from Xigaze ophiolite: Abundance of serpentine in slow spreading ridge. *Geophysical Research Letters*, **23**, 9-12.

Iyer, K., Austrheim, H., John, T. and Jamtveit, B., 2007a. Serpentinization of the oceanic lithosphere and some geochemical consequences: Insights from the Leka Ophiolite Complex, Norway. *Chemical Geology*, in review.

Iyer, K., Jamtveit, B., Mathiesen, J., Malthe-Sørenssen, A. and Feder, J., 2007b. Reaction-assisted hierarchical fracturing during serpentinization. *Earth and Planetary Science Letters*, in review.

Jenkins, D. M., 1983. Stability and Composition Relations of Calcic Amphiboles in Ultramafic Rocks. Contributions to Mineralogy and Petrology, **83**, 375-384.

Karson, J. A., Thompson, G., Humphris, S. E., Edmond, J. M., Bryan, W. B., Brown, J. R., Winters, A. T., Pockalny, R. A., Casey, J. F., Campbell, A. C., Klinkhammer, G., Palmer, M. R., Kinzler, R. J and Sulanowska, M. M., 1987. Along-Axis Variations in Sea-Floor Spreading in the Mark Area. *Nature*, **328**, 681-685.

Kelley, D. S., Karson, J. A., Blackman, D. K., Fruh-Green, G. L., Butterfield, D. A., Lilley, M. D., Olson, E. J., Schrenk, M. O., Roe, K. K., Lebon, G. T. and Rivizzigno, P., 2001. An off-axis hydrothermal vent field near the Mid-Atlantic Ridge at 30°N. *Nature*, **412**, 145-149.

Kelley, D. S., Karson, J. A., Fruh-Green, G. L., Yoerger, D. R., Shank, T. M., Butterfield, D. A., Hayes, J. M., Schrenk, M. O., Olson, E. J., Proskurowski, G., Jakuba, M., Bradley, A., Larson, B., Ludwig, K., Glickson, D., Buckman, K., Bradley, A. S., Brazelton, W. J., Roe, K., Elend, M. J., Delacour, A., Bernasconi, S. M., Lilley, M. D., Baross, J. A., Summons, R. T. and Sylva, S.

P., 2005. A serpentinite-hosted ecosystem: The lost city hydrothermal field. *Science*, **307**, 1428-1434.

Komor, S. C., Elthon, D. and Casey, J. F., 1985. Serpentinization of Cumulate Ultramafic Rocks from the North Arm Mountain Massif of the Bay of Islands Ophiolite. *Geochimica Et Cosmochimica Acta*, **49**, 2331-2338.

Kyser, T. K. and Kerrich, R., 1991. Retrograde exchange of hydrogen isotopes between hydrous minerals and water at low temperatures. *In: Taylor H. P., Jr, O'Neil, J. R. and Kaplan, I. R. (eds.). Stable Isotope Geochemistry: a tribute to Samual Epstein, The Geochemical Society, Special Publication*, **3**, 409-424.

Laurent, R., 1980. Regimes of Serpentinization and Rodingitization in Quebec Appalachian Ophiolites. *Archives Des Sciences*, **33**, 311-320.

Le Gleuher, M., Livi, K. J. T., Veblen, D. R., Noack, Y. and Amouric, M., 1990. Serpentinization of Enstatite from Pernes, France: Reaction Microstructures and the Role of System Openness. *American Mineralogist*, **75**, 813-824.

Lister, C. R. B., 1974. On the penetration of water into hot rock. *Geophysical Journal of the Royal Astronomical Society*, **39**, 465-509.

Lowell, R. P. and Germanovich L. N., 1994. On the Temporal Evolution of High-Temperature Hydrothermal Systems at Ocean Ridge Crests. *Journal of Geophysical Research-Solid Earth*, **99**, 565-575.

Lowell, R. P. and Rona, P. A., 2002. Seafloor hydrothermal systems driven by the serpentinization of peridotite. *Geophysical Research Letters*, **29**, doi: 10.1029/2001GL014411.

MacDonald, K. C., 1982. Mid-Ocean Ridges - Fine Scale Tectonic, Volcanic and Hydrothermal Processes within the Plate Boundary Zone. *Annual Review of Earth and Planetary Sciences*, **10**, 155-190.

MacDonald, A. H. and Fyfe, W. S., 1985. Rate of Serpentinization in Seafloor Environments. *Tectonophysics*, **116**, 123-135.

Martin, B. and Fyfe, W. S., 1970. Some experimental and theoretical observations on the kinetics of hydration reactions with particular reference to serpentinization. *Chemical Geology*, **6**, 185-202.

Melekhova, E., Schmidt, M. W., Ulmer, P. and Guggenbühl, E., 2006. The reaction talc + forsterite = enstatite + H_2O revisited: Application of conventional and novel experimental techniques and derivation of revised thermodynamic properties. *American Mineralogist*, **91**, 1081-1088.

Mével, C., 2003. Serpentinization of abyssal peridotites at mid-ocean ridges. *Comptes Rendus Geoscience*, **335**, 825-852.

Mével, C., Cannat, M., Gente, P., Marion, E., Auzende, J. M. and Karson, J. A. 1991. Emplacement of Deep Crustal and Mantle Rocks on the West Median Valley Wall of the Mark Area (Mar, 23-Degrees-N). *Tectonophysics*, **190**, 31-53.

Miller, D. J. and Christensen, N. I., 1997. Seismic velocities of lower crustal and upper mantle rocks from the slow-spreading Mid-Atlantic Ridge, South of the Kane transform zone (MARK area). *Proceedings of the Ocean Drilling Program, Scientific Results, College Station, TX*, **153**, 437-454.

Moody, J. B., 1976. Serpentinization - Review. *Lithos*, **9**, 125-138.

Neal, C. and Stanger, G., 1983. Hydrogen Generation from Mantle Source Rocks in Oman. *Earth and Planetary Science Letters*, **66**, 315-320.

Nicolas, A., Mainprice, D. and Boudier, F., 2003. High-temperature seawater circulation throughout crust of oceanic ridges: A model derived from the Oman ophiolites. *Journal of Geophysical Research-Solid Earth*, **108**, doi:10.1029/2002JB002094.

O'Hanley, D. S., 1992. Solution to the volume problem in serpentinization. *Geology*, **20**, 705-708.

O'Hanley, D.S., 1996. Serpentinites: records of tectonic and petrological history. *Oxford Monographs on Geology and Geophysics*, **34**.

O'Hanley, D. S., Kyser, T. K. and Stauffer, M., 1993. Provenance, deformation, and alteration history of mafic-ultramafic rocks east of Amisk Lake, and the provenance of the mafic and ultramafic Boundary Intrusions, in the Flin Flon Domain, trans-Hudson Orogen. *Lithoprobe Report*, **34**, 190-206.

Oufi, O., Cannat, M. and Horen, H., 2002. Magnetic properties of variably serpentinized abyssal peridotites, *Journal of Geophysical Research*, **107**, doi: 10.1029/2001JB000549.

Pawley, A. R., 1998. The reaction talc + forsterite = enstatite + H_2O: New experimental results and petrological implication. *American Mineralogist*, **83**, 51-57.

Peacock, S. M., 1987. Serpentinization and Infiltration Metasomatism in the Trinity Peridotite, Klamath Province, Northern California - Implications for Subduction Zones. *Contributions to Mineralogy and Petrology*, **95**, 55-70.

Penrose Field Conference, 1972. Ophiolites. *Geotimes*, **17**, 24-25.

Pearce, J. A., Lippard, S. J. and Roberts, S., 1984. Characteristics and tectonic significance of supra-subduction zone ophiolites. *In: Kokelaar, B. P. and Howell, M. F. (eds.). Marginal basin geology, Geological Society of London, Special Publication*, **16**, 77-94.

Rona, P. A., Bougault, H., Charlou, J. L., Appriou, P., Nelsen, T. A., Trefry, J. H., Eberhart, G. L., Barone, A. and Needham, H. D., 1992. Hydrothermal Circulation, Serpentinization, and Degassing at a Rift-Valley Fracture-Zone Intersection - Mid-Atlantic Ridge near 15°N, 45°W. *Geology*, **20**, 783-786.

Saleeby, J., 1984. Tectonic significance of serpentine mobility and ophiolitic mélange. *Geological Society of America Special Paper*, **198**, 153-168.

Schroeder, T., John, B. and Frost, B. R., 2002. Geologic implications of seawater circulation through peridotite exposed at slow-spreading mid-ocean ridges. *Geology*, **30**, 367-370.

Shervais, J. W., Kolesar, P. and Andreasen, K., 2005. A field and chemical study of serpentinization-Stonyford, California: Chemical flux and mass balance. *International Geology Review*, **47**, 1-23.

Sherwood-Lollar, B., Frape, S. K., Weise, S. M., Fritz, P., Macko, S. A. and Welhan, J. A., 1993. Abiogenic methanogenesis in crystalline rocks. *Geochimica Et Cosmochimica Acta*, **57**, 5087-5097.

Thurnherr, A. M. and Richards, K. J., 2001. Hydrography and high-temperature heat flux of the Rainbow hydrothermal site (36°14′N, Mid-Atlantic Ridge). *Journal of Geophysical Research-Oceans*, **106**, 9411-9426.

Tivey, M. K., 2007. Generation of Seafloor Hydrothermal Vent Fluids and Associated Mineral Deposits. *Oceanography*, **20**, 50-65.

Toft, P. B., Arkani-Hamed, J. and Haggerty, S. E., 1990. The effects of serpentinization on density and magnetic susceptibility: a petrophysical model. *Physics of the Earth and Planetary Interiors*, **65**, 137-157.

Uehara, S. and Shirozu, H., 1985. Variations in chemical compositions and structural properties of antigorite. *Mineralogical Journal*, **12**, 299-318.

Viti, C., Mellini, M. and Rumori, C., 2005. Exsolution and hydration of pyroxenes from partially serpentinized harzburgites. *Mineralogical Magazine*, **69**, 491-507.

Watanbe, T., Oguri, H., Yano, H. and Yoneda, A., 2007. Compressional and shear wave velocities in serpentinized peridotites. *American Geophysical Union, Fall Meeting (Abstract), San Francisco*, Ref. no. 671.

Wetzel, L. R. and Shock, E. L., 2000. Distinguishing ultramafic- from basalt-hosted submarine hydrothermal systems by comparing calculated vent fluid compositions. *Journal of Geophysical Research-Solid Earth*, **105**, 8319-8340.

Wicks, F. J. and Plant, A. G., 1979. Electron-microprobe and X-ray microbeam studies of serpentine textures. *Canadian Mineralogist*, **17**, 785-830.

Wicks, F. J. and Whittaker, E. J. W., 1975. A reappraisal of the structure of serpentine minerals. *Canadian Mineralogist*, **13**, 227-243.

Wicks, F. J. and Whittaker, E. J. W., 1977. Serpentine textures and serpentinization. *Canadian Mineralogist*, **15**, 459-488.

Wirth, K. R. and Bird, J. M., 1994. Chronology of ophiolite crystallization, detachment, and emplacement: evidence from the Brooks range, Alaska. *Geology*, **20**, 75-78.